volume of aluminium. The same is true for our phase as well (15.19 Å^3 for CaF_2-type and 22.97 Å^3 for diamond cubic type).

Further proof that we are dealing with isostructural metastable phases in both Al–Fe and Al–Pt systems can be obtained from diffraction patterns (Fig. 1b). If we consider the intense spots, then it will be observed that this pattern is the same as that reported by Stowell and co-workers in Fig. 8c of their paper [2]. The schematic illustration of their pattern also holds good for our pattern and we can, therefore, conclude that the same orientation relationship exists in both cases, namely

(1 1 1) precipitate ‖ (0 0 1) matrix

[$\bar{1}$ 1 0] precipitate ‖ [0 1 0] matrix

In order to understand the missing 2 0 0 reflection, we have carried out structure factor calculations for electron diffraction for the first three reflections. The results are shown in Table I. In both cases (Al_2Fe and Al_2Pt) we have considered the atom positions as in CaF_2 [3]. It can be seen that the intensity of the 2 0 0 reflection is much less in comparison to other reflections. Since the 2 0 0 reflection occurs very near to the strong 1 1 1 reflection, it is likely that it may not be seen in the electron diffraction patterns.

TABLE I Calculated structure factors of Al_2Pt and Al_2Fe metastable phases for electron diffraction.

hkl	$\lvert F\rvert^2$	
	Al_2Pt	Al_2Fe
1 1 1	1425	340
2 0 0	145	30
2 2 0	1770	760

Note added in proof

An isostructural metastable Al_2Pd phase has since been observed in a rapidly solidified Al–6 at% Pd alloy (G.V.S. Sastry and C. Suryanarayana, private communication).

Acknowledgements

The authors thank Professor T. R. Anantharaman and Professor S. L. Malhotra for encouragement throughout the work. The financial grant from the University Grants Commission, New Delhi is gratefully acknowledged.

References

1. R. HUCH and W. KLEMM, *Z. anorg. Chem.* **329** (1964) 123.
2. M. H. JACOBS, A. G. DOGGETT and M. J. STOWELL, *J. Mater. Sci.* **9** (1974) 1631.
3. W. B. PEARSON, "The Crystal Chemistry and Physics of Metallic Alloys" (Wiley Interscience, New York, 1972) p. 385.

Received 8 March
and accepted 2 May 1978.

K. CHATTOPADHYAY
S. LELE
P. RAMACHANDRARAO
Department of Metallurgical Engineering,
Banaras Hindu University,
Varanasi, India.

A novel method for the establishment of solvus surfaces as demonstrated with nickel-base alloys

The unidirectional solidification of alloys in the form of dendritic monocrystals, followed by quenching of the remaining liquid at a given moment, offers a very broad spectrum of possible microstructural studies as a function of temperature and time. In polyphase alloys the process allows the determination of the temperature at which a given phase appears and of the temperature range over which it grows. It also makes it possible, knowing the constant rate at which the dendritic monocrystal is pulled, to study growth or coarsening kinetics of the various phases.

In cast nickel-base alloys γ' precipitates in the solid at the solvus temperatures, which depends on the local concentration of those elements that are included in this phase. Based on this precipitation a novel method is described herein for the establishment of solvus surfaces and is applied to the ternary Ni–Al–Ta system.

Dendritic monocrystals of Ni–7.5 wt% Al–2.0 wt% Ta, Ni–8.0 wt% Al–2.0 wt% Ta and Ni–8.5 wt% Al–2.0 wt% Ta were unidirectionally solidifed under argon in an induction furnace

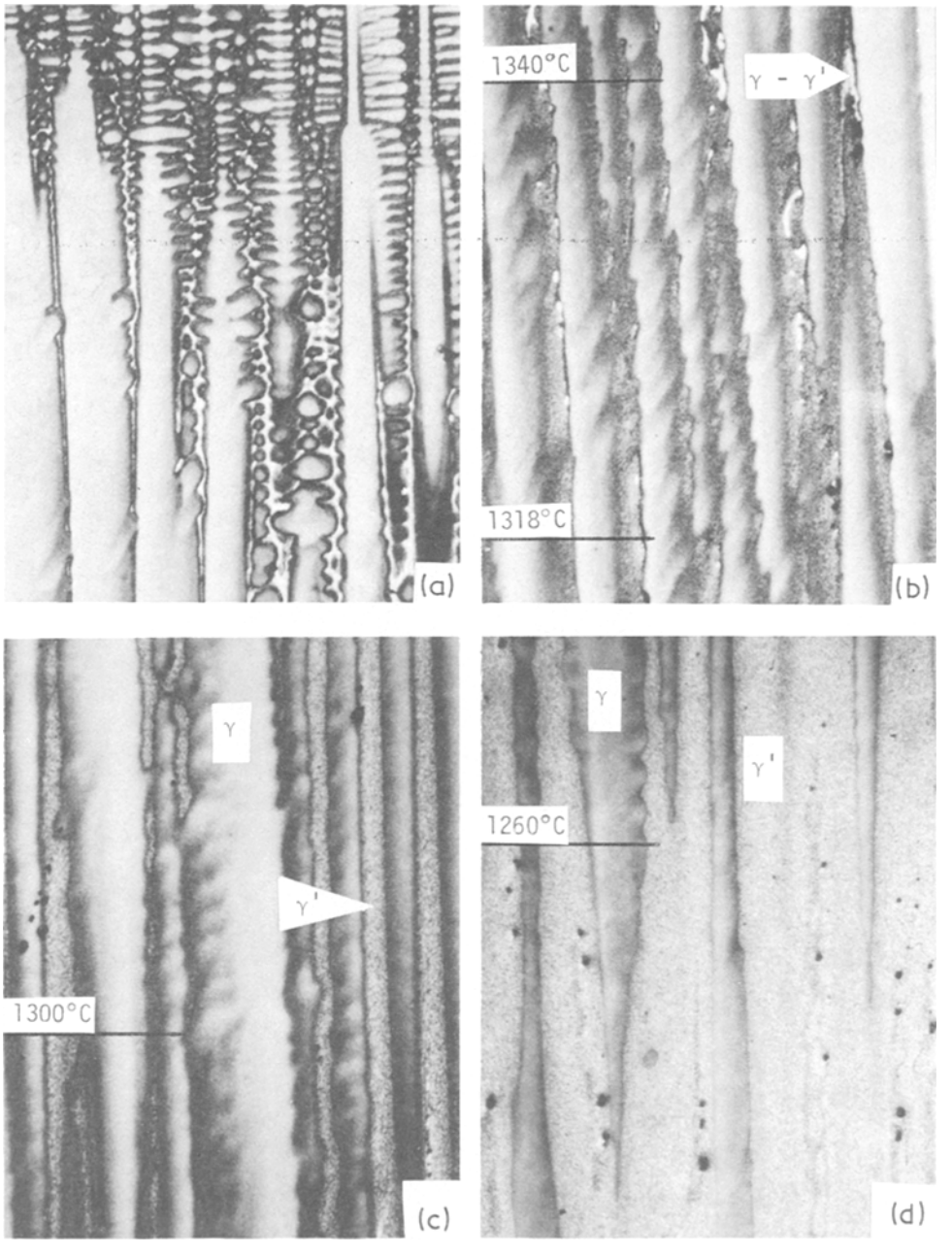

Figure 1 Successive photomicrographs of a longitudinal section of a dendritic monocrystal of Ni–8.5% Al–2.0% Ta, taken at increasing distances from the quenched interface. Ingot continuously grown at 0.25 m h^{-1} before quenching (× 43).

equipped with a water-cooled bottom [1]. The drop-cast master alloy was placed in a tubular alumina crucible (0.005 m i.d. × 1.00 m long) and was indirectly heated, using a graphite susceptor in order to avoid induction stirring of the melt. The crucible was lowered at a uniform rate of 0.25 m h^{-1}. For this particular set-up the rate at which the crucible was pulled was equal to the growth rate of the solid. This growth rate, $R = 0.25$ m h^{-1} and the average thermal gradient in the solid–liquid region, $G \approx 6 \times 10^3$ °C m^{-1}, were selected so that growth of the solid was

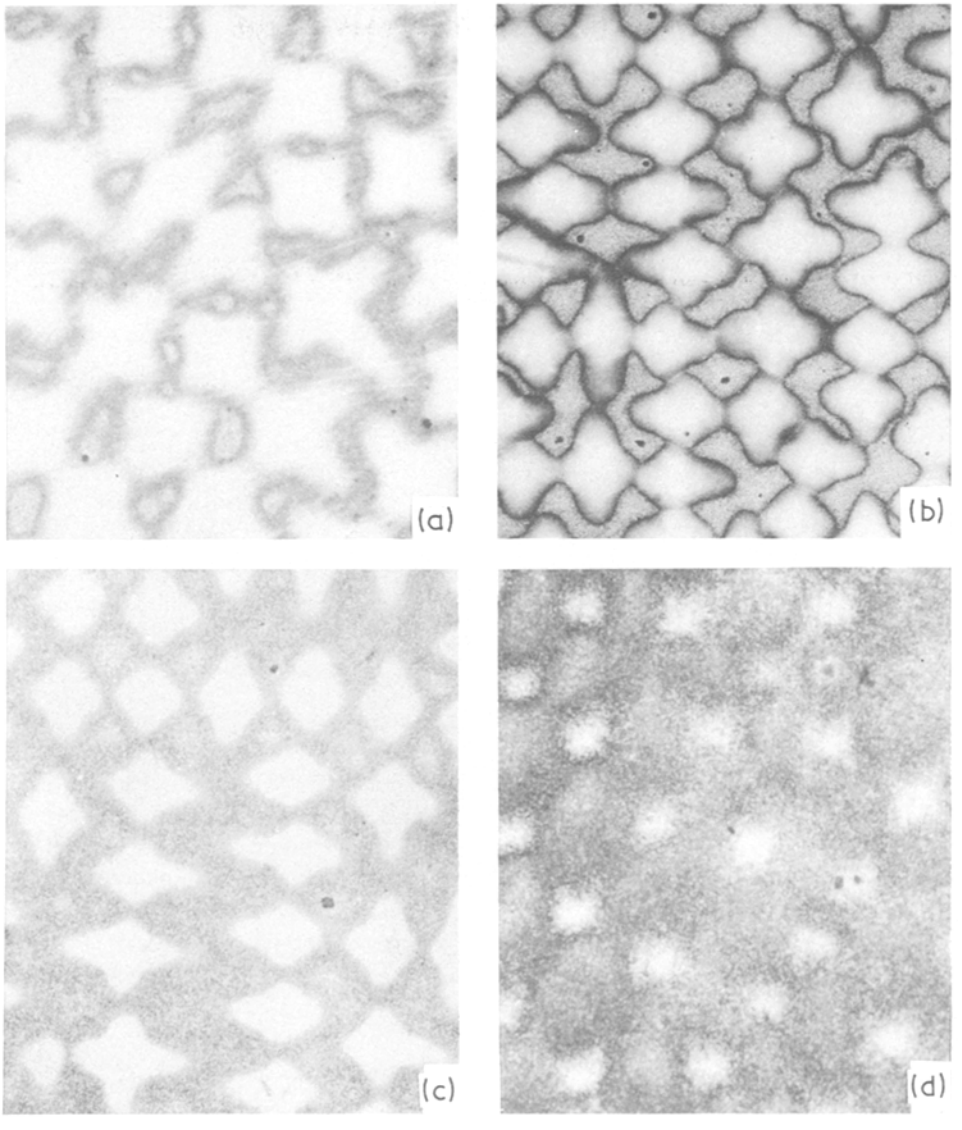

Figure 2 Photomicrographs of transverse sections of a dendritic monocrystal of Ni–8.5% Al–2.0% Ta, taken at increasing distances from the quenched interface, and hence at decreasing temperatures. Ingot continuously grown at 0.25 m h^{-1} before quenching. Corresponding temperatures are: (a) 1340° C, (b) 1318° C, (c) 1300° C and (d) 1260° C, as indicated in Fig. 1 (× 43).

dendritic. A 17 kW power supply of medium frequency (0.5 MHz) was used. Growth of the solid was interrupted at a given moment by stopping the downward motion of the crucible for about 1 min in order to attain equilibrium between the various phases at different temperatures. The remaining liquid was finally quenched by pneumatically pulling the crucible out of the furnace at very high speed.

An axially inserted thermocouple gave the temperature variation with time, hence with location since the solid was pulled at constant rate. The liquidus temperature at the dendrite tips for each alloy was taken as the temperature of appearance of the dendritic solid and was determined by differential thermal analysis. For this purpose a SETARAM-2400 K analyser was used, equipped with a high temperature (2400 K) cell, under argon atmosphere. Thus, the temperature at a given location at the moment of quench could be finally determined.

The microstructure of a dendritic monocrystal

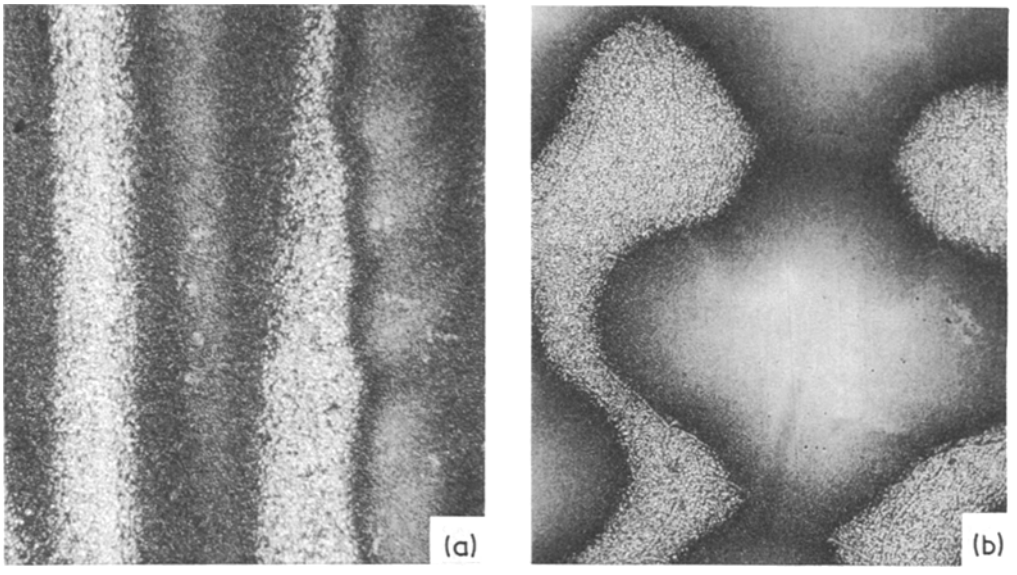

Figure 3 Photomicrographs of longitudinal (a) and transverse (b) sections of a dendritic monocrystal of Ni–8.5% Al–2.0% Ta grown at 0.25 m h^{-1} before quenching. The transverse section corresponds to a temperature of 1318° C. (× 400).

after quenching is illustrated in Fig. 1, which contains photomicrographs of the longitudinal section corresponding to various distances from the dendrite tips, increasing from Fig. 1a to Fig. 1d. Fig. 1b illustrates the last interdendritic γ–γ' eutectic pools. The eutectic is solutionized and disappears beyond a certain distance from the dendrite tips, hence below a temperature of about 1330° C. Fig. 1b also illustrates the appearance of γ', precipitated during continuous growth of the monocrystal at 0.25 m h^{-1} in the interdendritic regions, where aluminium and tantalum concentrations are maximum. The precipitation most likely continued and was completed during the 1 min arrest, as can be assumed from published information on precipitation kinetics of γ' in γ [2]. The duration of the arrest could of course be lengthened beyond the 1 min. At still lower temperatures, Figs. 1c and d, the zones within which γ' has precipitated become wider. The extent of these zones is better illustrated in Fig. 2 which exhibits transverse sections of the monocrystal taken within the solid at different locations and temperatures, as reported in Figs. 1b to d. A second generation of finer γ' can sometimes be optically resolved within the rest of the dendritic solid, Figs. 3a and b. This very fine γ' formed during quenching. The boundary limiting the region of coarser γ' precipitation is an isoconcentration surface [3] in aluminium and tantalum. With decreasing temperature this boundary shifts towards the dendritic centre-line and the corresponding aluminium and tantalum concentrations decrease. The temperature variation versus the concentration of aluminium or tantalum which correspond to the boundary is precisely the solvus curve with respect to each one of these two alloying elements.

A new method for the establishment of the solvus curves of an alloy then results from the previous considerations. This method was applied to the Ni–Al–Ta system: a series of transverse sections was made in a dendritic monocrystal of each one of the three compositions, at known distances from the dendrite tips, Fig. 2. The temperature for each section at the moment of quench was deduced from the measured temperature versus distance variation combined with the value of the temperature at the dendrite tips, measured by DTA. The concentration of aluminium and tantalum along the boundary of the γ'-precipitated regions was then determined by electron microprobe analysis, using the point counting technique. Temperature was finally plotted versus aluminium concentration, Fig. 4a, and tantalum concen-

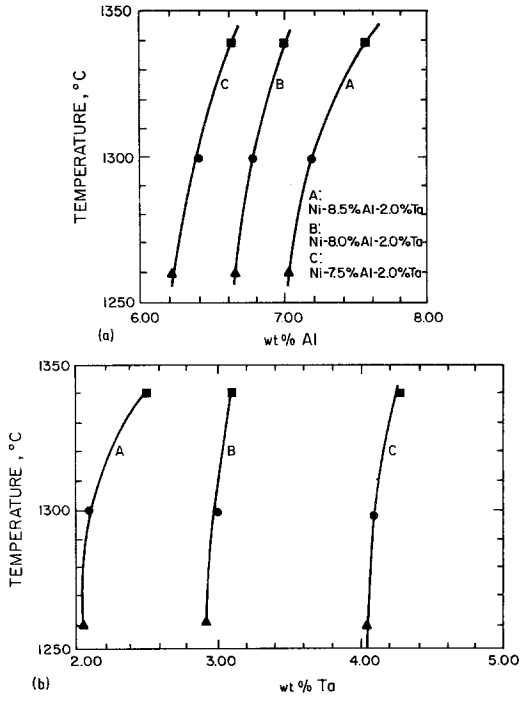

Figure 4 Solvus curves of the three alloys versus wt% Al and wt% Ta.

tration, Fig. 4b. Information from Fig. 4 was replotted in Fig. 5, which exhibits basal projections of isothermal intersections of the solvus surface at three different temperatures, 1340° C, 1300° C and 1260° C. For comparison purposes, solvus points for the Ni–Al binary system [4] corresponding to these temperatures have been indicated on the same diagram. No other information on the solvus surface of the Ni–Al–Ta system in the nickel corner has been found available for further comparison.

It is difficult to compare the accuracy of the method described herein with that of classical methods used for determining solvus curves. These methods involve alloy preparation, homogenization, heat treatment and quenching from various temperatures, followed by X-ray diffraction analysis, optical microscopic examination or electron microprobe analysis. The accuracy of the "disappearing-phase" method [5] depends on the sensitivity of the X-ray method used for detecting small amounts of a secondary phase in a mixture, which in turn depends greatly on the alloy. If the secondary phase is detected by optical microscopy accuracy may be improved [5]. Also, the sensitivity of the microscope is independent of the atomic numbers of the elements involved; however, it depends on the particle size of the secondary phase. The "parametric method" [5] is more accurate than the disappearing-phase method, whether based on X-ray measurements or microscopic examination. The accuracy of the method proposed in this paper depends on: (1) that involved in determining the liquidus temperature by DTA; (2) that involved in establishing the dependence of temperature on time or distance; (3) that involved in defining the boundary which limits the γ'-precipitated region. A fast quench yields well-defined boundaries, and; (4) that involved in measuring solute concentrations at this boundary by electron microprobe analysis. It is estimated that an error of ± 3° C may affect the temperature measurement and a relative error of up to ± 5%, the concentration measurement.

The main advantage of the proposed method which obviously can be applied to other systems is its simplicity and rapidity. A solvus curve, Fig. 4, can be plotted from one dendritic monocrystal of a given composition. The extent of each curve in Fig. 5 depends on the number of dendritic monocrystals of different compositions which were grown, whereas the number of these curves depends simply on the number of isothermal sections which were made in the original monocrystal.

A method is proposed herein for establishing solvus surfaces and is applied to the ternary

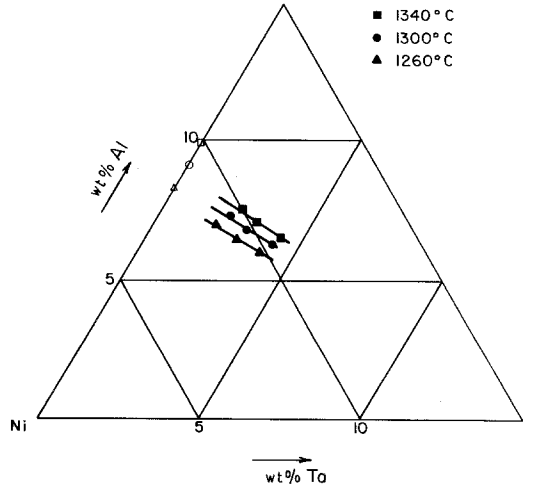

Figure 5 Isothermal solvus curves at three different temperatures. Ni–Al–Ta alloy system. Hollow points on the Ni–Al axis are from Hansen *et al.* [4].

Ni–Al–Ta system. Dendritic monocrystals of various compositions are sectioned at different locations from the quenched interface and temperature at the moment of quench, corresponding at the boundaries limiting the γ'-precipitated regions are subsequently established by electron microprobe analysis. Temperature is finally plotted versus concentration of each solute and results are reported on the ternary diagram.

The accuracy of the method is estimted to ± 3° C in temperature and ± 0.05 of 1% in concentration. The method is general in nature, rapid and allows the construction of a solvus curve with only one dendritic monocrystal of a given composition.

Acknowledgements

Support of this project by an Air Force Office of Scientific Research Grant No. 77-3344 to the University of Connecticut is gratefully acknowledged. Part of the work was carried out at the Centre des Matériaux, E.N.S.M.P. during a sabbatical leave of one of the authors (TZK).

References

1. J. C. LECOMTE and G. LESOULT, Proceedings of the 20th Colloque de Métallurgie (1977) Centre d'Etudes Nucléaires de Saclay Gif-sur-Yvette, France, p. 415.
2. R. F. DECKER, Proceedings of the Climax Molybdenum Symposium, Zurich, Switzerland (1969).
3. T. Z. KATTAMIS and M. C. FLEMINGS, *Trans. TMS-AIME* **233** (1965) 992.
4. M. HANSEN and K. ANDERKO, "Constitution of Binary Alloys" (McGraw-Hill Book Company, New York, 1958).
5. B. D. CULLITY, "Elements of X-ray Diffraction" (Addison–Wesley Publishing Company, Inc., Reading, Massachusetts, 1959).

Received 15 March
and accepted 3 May 1978.

T. Z. KATTAMIS
Department of Metallurgy,
Institute of Materials Science,
University of Connecticut,
Storrs, Connecticut 06268, USA
J. C. LECOMTE
Framatome,
Chalon-sur-Sâone, France

New magnesium hydroxynitrate hydrate binder

Nitrate-based magnesia cements have been rarely reported [1, 2], and only one magnesium hydroxynitrate composition, $Mg_3(OH)_4(NO_3)_2$, has been defined [3] – resulting from thermal decomposition of $Mg(NO_3)_2 \cdot 6H_2O$ above 300° C.

This study was undertaken to examine nitrate-based cements formed from magnesia (MgO) powder. The MgO powder was ≥ 99.86 wt% pure by spark-source mass spectrometry, and had a mean particle diameter of 4.2 μm. The solutions used were reagent grades of $Mg(NO_3)_2$, NH_4NO_3, or HNO_3 and are shown in Table I along with observations of cement formation. The MgO powder (pre-calcined at 600° C) was mixed with the appropriate solution in a glass beaker. The liquid volume in cm^3 to powder weight in grams (or L/P) ratios adequately define the compositions used. After mixing, the beakers were held by a larger beaker in a sealed container of saturated $(NH_4)_2SO_4$ solution which provided a curing environment with a fixed 81.1% relative humidity. Samples were inspected frequently for 72 h and intermittently observed for 2 weeks. Afterwards, samples were dried at 50° C for 24 to 48 h, and examined by X-ray diffraction (XRD).

Table I shows that the same phase (unknown "X") occurs for all $Mg(NO_3)_2$ additions to MgO. Only slight variations in intensity occurred in the XRD patterns. The cements which set and could be dried without cracking (Nos. 1 and 2) were analysed chemically and by mercury intrusion porosimetry, with the data presented in Table II.

Since the predominant phase from HNO_3 or NH_4NO_3 reactions is $Mg(OH)_2$, and since there is considerably less NO_3^- present in the dried cements than initially used, it appears that some nitrogen components (such as N_2O, NO, NO_2) must be evolved in the formation of the binder, such that its final composition is approximately constant whenever $Mg(NO_3)_2$ salt solutions are used. The slight intensity variations in the XRD data probably result from variable water content. The $Mg(OH)_{1.8}(NO_3)_{0.2} \cdot 1.55\ H_2O$ binder phase XRD pattern is shown in Table III.

Examination of the cementitious $Mg(NO_3)_2$-produced materials by scanning electron microscopy showed the binders to be needles (1 to 15 μm